

## Research Article

## Open Access

M. Ajay Kumar\* and N.V. Srikanth

# An Adaptive Coordinated Control for an Offshore Wind Farm Connected VSC Based Multi-Terminal DC Transmission System

**Abstract:** The voltage source converter (VSC) based multi-terminal high voltage direct current (MTDC) transmission system is an interesting technical option to integrate offshore wind farms with the onshore grid due to its unique performance characteristics and reduced power loss via extruded DC cables. In order to enhance the reliability and stability of the MTDC system, an adaptive neuro fuzzy inference system (ANFIS) based coordinated control design has been addressed in this paper. A four terminal VSC-MTDC system which consists of an offshore wind farm and oil platform is implemented in MATLAB/SimPowerSystems software. The proposed model is tested under different fault scenarios along with the converter outage and simulation results show that the novel coordinated control design has great dynamic stabilities and also the VSC-MTDC system can supply AC voltage of good quality to offshore loads during the disturbances.

**Keywords:** Offshore wind, VSC HVDC, ANFIS, Coordinated controller, MTDC, MATLAB.

DOI 10.1515/eng-2015-0005

Received July 05, 2014; accepted October 13, 2014

## 1 Introduction

Nowadays, with the growth in HVDC transmission, voltage source converter (VSC) based HVDC also known as “HVDC Light” transmission system has become more and more important in the larger interconnected power system [1]. The main advantage of HVDC Light over conventional HVDC is that the extension to multi-terminal DC (MTDC) systems is relatively easy and hence, the applica-

tion of MTDC systems is becoming more attractive than before. The VSC based MTDC system is better than the two-terminal HVDC system in several aspects like reliability, control flexibility and economics [2, 3]. One essential application of VSC based MTDC transmission system is to interconnect offshore wind farms and oil/gas platforms to the onshore grid, which will reduce the operational costs and increase the reliability. Although, there are no VSC based MTDC systems installed so far, a large number of publications existed in the area of VSC based MTDC. All these research works concentrate on different aspects such as DC fault location and protection of MTDC [4], control methodologies [2, 5], and also modeling of MTDC [6].

MTDC systems for power transmission between conventional AC networks and DFIG based wind farms were described in [2, 7]. In [8], a three terminal VSC based HVDC system connecting onshore AC grid to two offshore wind farms was introduced and analyzed. Recently, a four terminal MTDC system was developed [9] where two onshore AC grids located at different geographical areas were integrated by two offshore wind farms and the DC grid control strategy and power sharing were clearly depicted. The operation of single or multi-terminal offshore system topologies were analyzed in [10] with the main focus on dynamic and transient simulations for numerous perturbations, including changes in wind speeds and short circuit faults like single phase to ground fault and three phase to ground fault at onshore and offshore AC grids. Recently, G. P. Adam et al. [11] proposed a novel control scheme termed as inertia emulation control for offshore wind farm grid integration, which enables the HVDC Light system to provide support that emulates the inertia of a synchronous generator. Inertia control scheme allows HVDC Light system with a fixed capacitance to emulate a wide range of inertia constants by specifying the amount of permissible DC voltage variation.

However, as far as control of MTDC system is concerned, the mentioned research was constrained to the conventional coordinated control design only [12]. In this paper, ANFIS based intelligent coordinated controller is imple-

\*Corresponding Author: M. Ajay Kumar: Department of Electrical Engineering, National Institute of Technology Warangal, India, E-mail: ajaykumar22@nitw.ac.in

N.V. Srikanth: Department of Electrical Engineering, National Institute of Technology Warangal, India

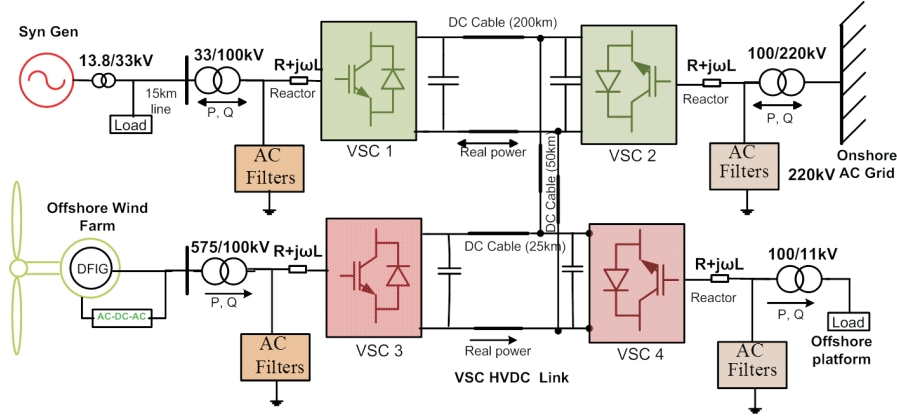


Figure 1: MTDC system for offshore wind farm and oil platform interconnection.

mented for the first time in MTDC systems, which does not require any mathematical modeling [13]. Moreover, the proposed controller gives fast response with a good quality of supply to offshore platforms with great dynamic stability.

The rest of the paper is organized as follows: Section 2 explains the complete MTDC system modeling and different controllers including the proposed controller. Simulation study at different perturbations and the results are discussed in section 3. At last, conclusions are presented in section 4.

## 2 MTDC system model

The Multi-terminal VSC based HVDC system tested in this paper is shown in Figure 1. It consists of four terminals in which VSC1 is connected to a conventional power plant feeding power to a strong AC grid through the second terminal VSC2 via DC link, the third terminal VSC3 is connected to an offshore DFIG based wind farm transmitting power to the onshore grid via DC cables and the fourth converter (VSC4) links to the offshore platforms supplying power through the DC link.

The main objectives of controlling MTDC system is not only to improve the overall performance of the system, but also to protect the equipment which is in service. VSCs play a vital role in the safe operation of the MTDC system. VSC1 controls the active power and reactive power whereas VSC2 adopts a DC voltage control method. But the wind farm side converter VSC3 must use constant active power and AC voltage, using power independent control systems. Finally, the converter connected to the oil platform (VSC4) is adopted with the AC voltage control method in order to

provide uninterrupted and balanced AC voltage at the terminal. Each VSC of the four terminal MTDC system is coupled with AC network via line resistor  $R$ , phase reactor  $L$  and a DC capacitor  $C$  is in parallel to the DC bus of the station as shown in Figure 1. The following equations are obtained in the d-q synchronous frame [14].

$$V_{sd} - V_{cd} = L \frac{di_d}{dt} + Ri_d + \omega Li_q \quad (1)$$

$$V_{sq} - V_{cq} = L \frac{di_q}{dt} + Ri_q - \omega Li_d \quad (2)$$

where  $V_{sd}$  and  $V_{sq}$  are source voltages,  $i_d$  and  $i_q$  are line currents,  $V_{cd}$  and  $V_{cq}$  are converter input voltages. Based on the instantaneous power theory, neglecting the losses of the converter and the transformer, the active and reactive power exchanges from the AC end of the DC link are:

$$P_{ac} = \frac{3}{2} (V_{sd}i_d + V_{sq}i_q) \quad (3)$$

$$Q_{ac} = \frac{3}{2} (V_{sd}i_q - V_{sq}i_d) \quad (4)$$

Suppose, the direction of the source voltage vector as d-axis,  $V_{sq} = 0$ . So Eq. (3) and (4) can be re-written as:

$$P_{ac} = \frac{3}{2} V_{sd}i_d \quad (5)$$

$$Q_{ac} = \frac{3}{2} V_{sd}i_q \quad (6)$$

Since  $V_{sd}$  is constant, from Eq. (5) and (6) it is clear that the active power will be controlled by  $i_d$ , whole reactive power will be controlled by  $i_q$ . On the DC side of the converter, DC current and DC power are:

$$i_{dc} = C \frac{dv_{dc}}{dt} + i_c \quad (7)$$

$$P_{dc} = V_{dc}i_{dc} \quad (8)$$

where  $i_{dc}$  is the DC current to be followed by the capacitor,  $v_{dc}$  is the DC link voltage and  $i_c$  is the current on the DC cable. Neglecting the loss of converter, power of AC side equals to the DC side.

$$P_{ac} = P_{dc} \quad (9)$$

$$\frac{3}{2}V_{sd}i_d = V_{dc}i_{dc} \quad (10)$$

Based on the law of conservation of energy, the active power transferred in the MTDC system must satisfy the following equation:

$$P_1 + P_2 + P_3 + P_4 = 0 \quad (11)$$

In MTDC system, each VSC is controlled by local controller and the whole system is coordinated by the master controller. Now, the control methodologies of MTDC system are briefly discussed as follows:

### A. Outer Controllers

In general, constant active, reactive power control and constant AC/DC voltage control strategy can be adopted for local control at each VSC of the MTDC system. Control circuit of each VSC is identical as shown in Figure 2 which consists of an outer control loop and inner current control loop. The outer controller includes the active, reactive power control, DC/AC voltage controller. The choice among these controllers will depend on the application. The outer controller will calculate the reference values of the converter current.

From the equations (5) and (6), it is clear that every converter can control its active and reactive power independently. A combination of an open loop and PI controller is used to keep the active power to its desired value, given by the equation:

$$i_{sd\_ref} = \frac{P_{Ref}}{V_{sd}} + \left( K_p + \frac{K_i}{s} \right) (P_{ref} - P) \quad (12)$$

Similarly, reactive power can also be controlled as in the previous case by combining the PI controllers as shown in below.

$$i_{sq\_ref} = \frac{Q_{ref}}{V_{sq}} + \left( K_p + \frac{K_i}{s} \right) (Q_{ref} - Q) \quad (13)$$

In general, the AC voltage controller is chosen at inverter station located on offshore oil platform so as to obtain an

uninterrupted and balanced AC voltage from the AC voltage controller, the d-axis current reference can be obtained using the equation:

$$i_{d\_ref} = \left( K_p + \frac{K_i}{s} \right) (v_{s\_ref} - v_s) \quad (14)$$

with

$$v_s = \sqrt{(v_{sd}^2 - v_{si}^2)} = v_{sd} \quad (15)$$

$$i_{d\_ref} = \left( K_p + \frac{K_i}{s} \right) (v_{s\_ref} - v_{sd})$$

MTDC system should maintain a constant DC link voltage under normal conditions in order to satisfy the power balance equation. When the MTDC system active power is superflow, VSC2 sends back to the AC grid and in this way without any energy storage device, VSC2 acts as an energy buffer by encountering the switching losses and transmission losses. When a PI controller is used, the DC current reference of VSC2 can be written as

$$i_{dc\_ref} = \left( K_p + \frac{K_i}{s} \right) (v_{dc\_ref} - v_{dc}) \quad (16)$$

All these outer loop PI regulators calculate the reference value of the converter current vector ( $I_{ref\_dq}$ ), which is the input to the inner current control loop.

### B. Inner Current Controller

According to the equations (1) and (2), the currents of  $d$  and  $q$  axis can be controlled by  $V_{cd}$  and  $V_{cq}$  respectively. The Inner current loop block contains two PI regulators that will calculate the reference value of the converter voltage vector ( $V_{ref\_dq}$ ). By using clarke's transformation  $V_{ref\_dq}$  is transformed into  $V_{ref\_abc}$ , which is the input to the space vector pulse width modulation (SVPWM) block.

### C. ANFIS based Coordinated Controller

MTDC Structure is more complex due to the interconnection of more than two converters for the same DC bus. So, it is necessary to control the DC link voltage within acceptable limits to assure that all active power on the DC grid is transmitted into the AC grid/load. In order to ensure the stability and reliability of the MTDC system, ANFIS based coordinated control strategy is used as master control in this paper.

ANFIS is an adaptive network that is functionally equivalent to a fuzzy inference system, where the output has been obtained by using fuzzy rules on inputs. Figure 3 depicts a two - input- one - output ANFIS structure [15]. The two inputs are  $x_1$  (error) which was obtained as ( $V_{dc\_ref} \sim V_{dclink}$ ),  $x_2$  (change of error) and the output is a controlled

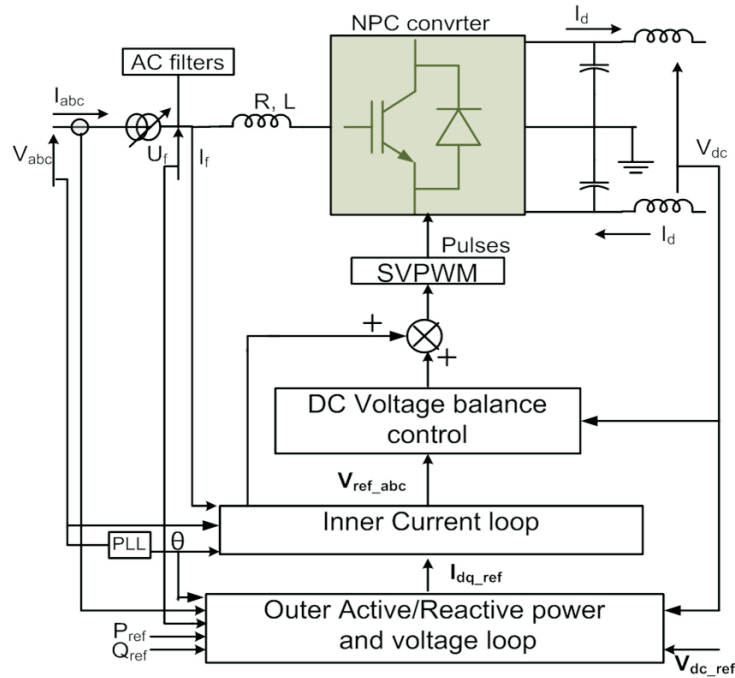


Figure 2: Control structure of a converter.

DC link voltage. Each input and output variable has five linguistic variables, i.e. Negative large (NL), Negative small (NS), Zero (Z), Positive small (PS) and Positive large (PL). Hence, in this proposed ANFIS controller total 25 linguistic variables are employed for getting the controlled output. The proposed ANFIS architecture consists of five layers wherein circle shaped nodes are called fixed nodes, which means the node parameters are independent on the other nodes and square shaped nodes are called adaptive nodes, whose node parameters depend on the other nodes [16]. Each neuron in the first layer corresponds to a linguistic variable while the output equals the membership function of this linguistic variable. In the second layer, each node multiplies the incoming signals and sends out the product that represents the firing strength of a rule. Each node in the third layer estimates the ratio of the rule firing strength to sum of the firing strength of all rules. In the fourth layer, the output is the product of the previously found relative firing strength of the  $i$ th rule. The final layer computes the overall output as the summation of the incoming signals. The proposed controller is checked in MATLAB/ANFIS editor tool box with a triangular membership function as it offers minimum training error. Since, the back propagation algorithm is notorious for its slowness and tendency to become trapped in local minima, a hybrid learning algorithm is used in this contribution. This algorithm is fast and accu-

Table 1: ANFIS parameters.

Number of nodes	75
Number of linear parameters	75
Number of nonlinear parameters	30
Total number of parameters	105
Number of training data pairs	600
Number of testing data pairs	100
Number of fuzzy rules	25

rate in identifying the parameters. The parameters of the ANFIS controller are given in Table 1.

### 3 Simulation and result analysis

In the test system as shown in Figure 1 the offshore wind farm consists of 133 units of DFIGs with a nominal power rating of 1.5MW each; accounting for a total capacity of 200 MW. The onshore AC grid is modeled as 1000 MVA, 220 kV voltage source. The offshore platform is modeled as a passive load of 100 MW. The test system was implemented in MATLAB/ Simulink and three case studies were carried out to demonstrate the feasibility of the controllers

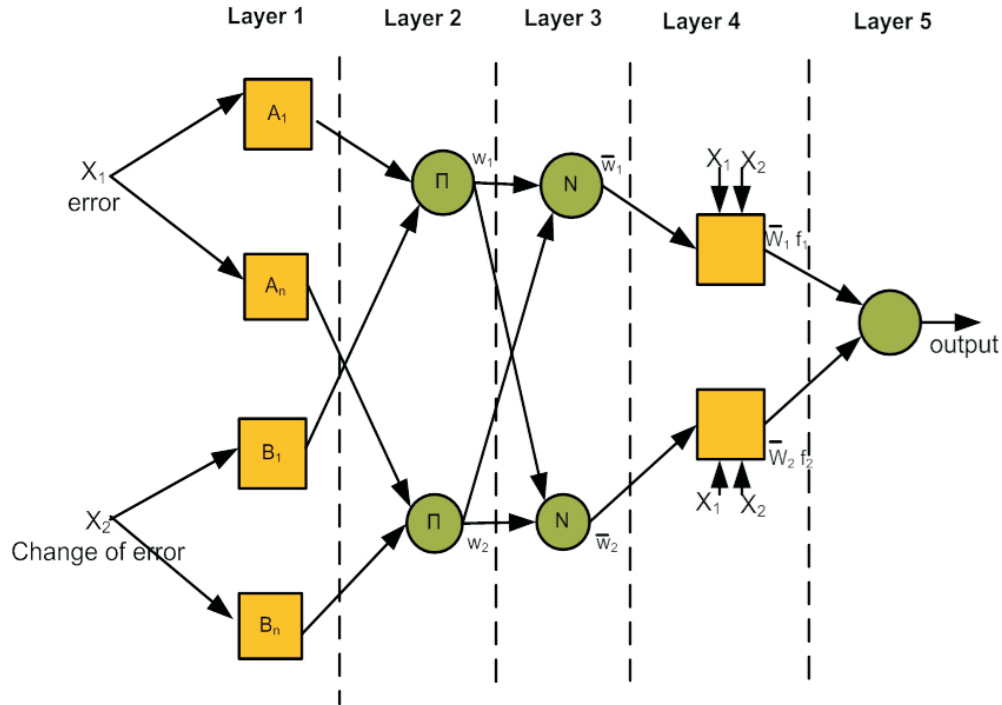


Figure 3: A Five layer ANFIS structure.

such as a three phase-to-ground fault on the grid side terminal, change in wind speed, and a temporary loss of one converter. Since, the fault on the AC side of VSC1 does not produce a destructive voltage surge and pose a great threat to the system stability; only the simulation results associated with an AC fault on the inverter side are presented. The dynamic responses of active power, reactive power, voltage and current along with the DC link parameters at all the terminals for different perturbations are shown in Figs. 4-6.

### 3.1 Three phase fault at an AC grid (Near VSC2)

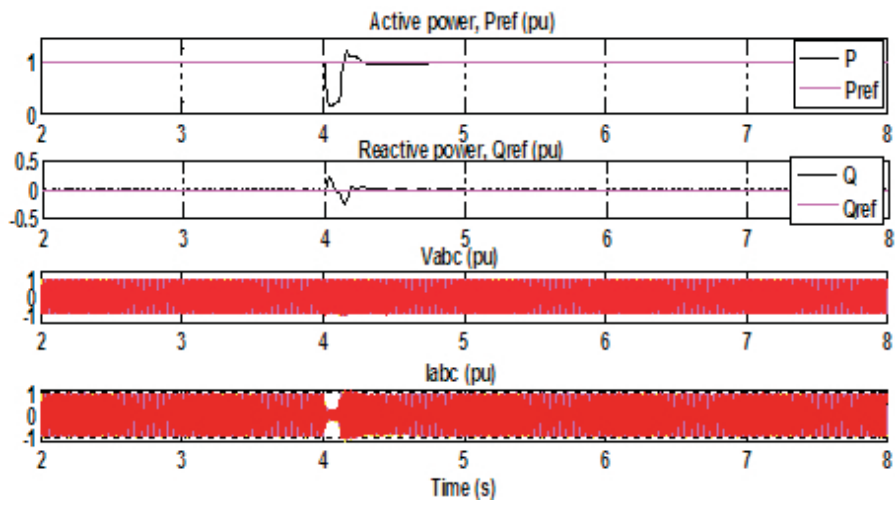
A balanced three phase fault was applied in an AC grid at 4s for a duration of 5-cycles to observe the effect of the proposed controller and simulation results were shown in Figure 4. It is clear from the Figure 4 (a) to (d) that, active power and reactive powers were quickly able to track their pre-defined values after removing the fault at an AC grid and during the fault there is a possibility of power transfer at all the VSCs except VSC2. Irrespective of the fault, the offshore wind farm is generating its rated power of 200 MW at a constant wind speed of 12 m/s as depicted in Fig-

ure 4 (e). The DC link voltage of MTDC system and power available at the DC side of the VSCs are shown in Figure 4 (f). Here, one can observe that the DC power transferred through VSC2 during the fault is zero and after the fault is cleared at 4.1 s, the VSC2 moves out of the current limit control mode and the DC link voltage oscillations were reduced in 10 ms as in Figure 4 (f).

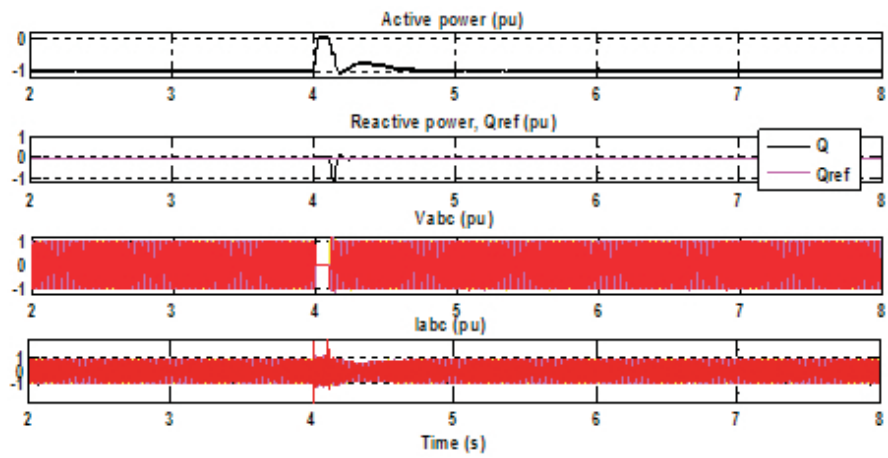
### 3.2 Change in wind speed

The second case study is based on the operation with change in the wind speed at the offshore power plant, and the results are shown in Figure 5. Initially, the wind speed is 12 m/s with generated power being around 200 MW from the DFIG wind farm. When the wind speed is decreased gradually to 10 m/s and back to 12 m/s for a span of 3 sec, a significant change in generating wind power of 140 MW and accordingly as shown in Figure 5 (f). Since, the VSC3 with fast energy storage can balance  $\pm 50$  MW fluctuations, irrespective of change in wind speed the active power and reactive powers at all the terminals are smooth and able to track their reference values as shown in Figure 5 (a) to (d). The DC power balance can be observed from Figure 5 (e).

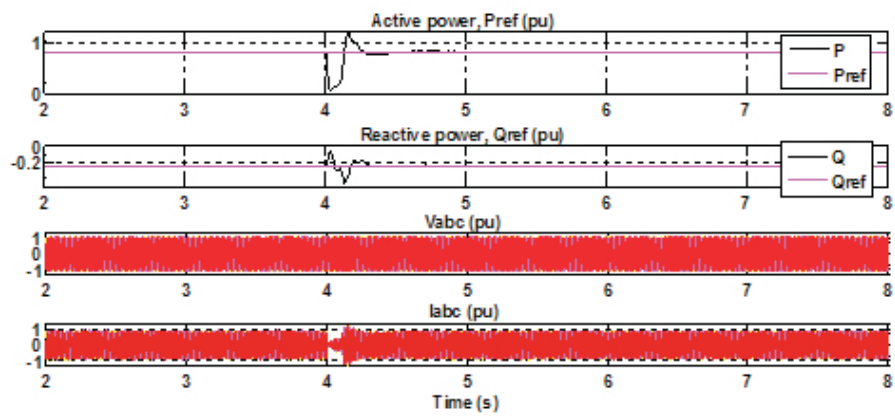
(a)



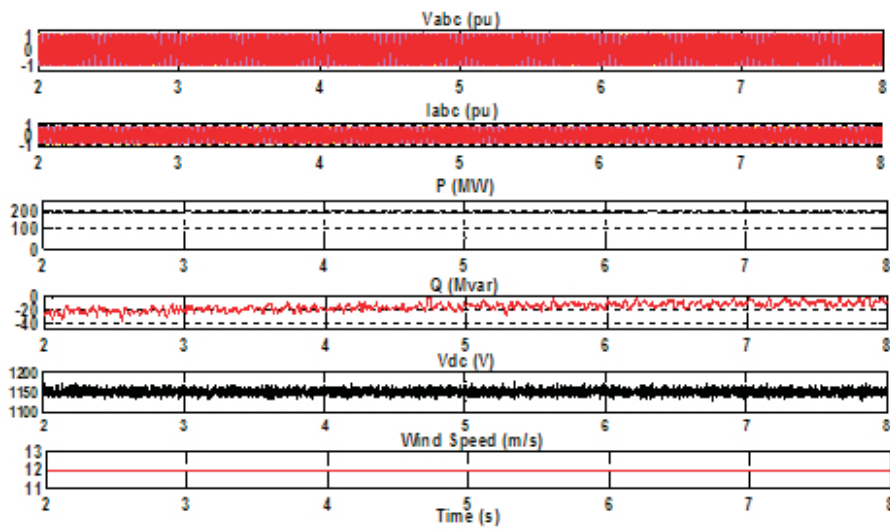
(b)



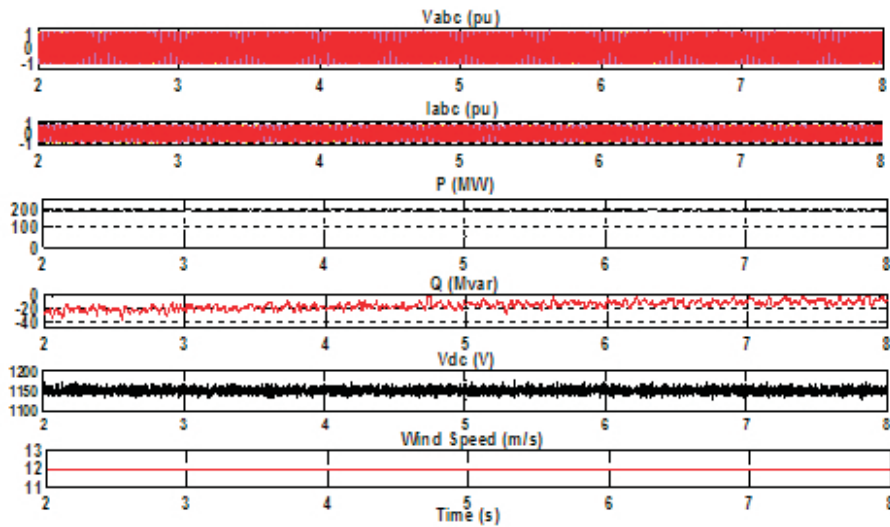
(c)



(d)



(e)



(f)

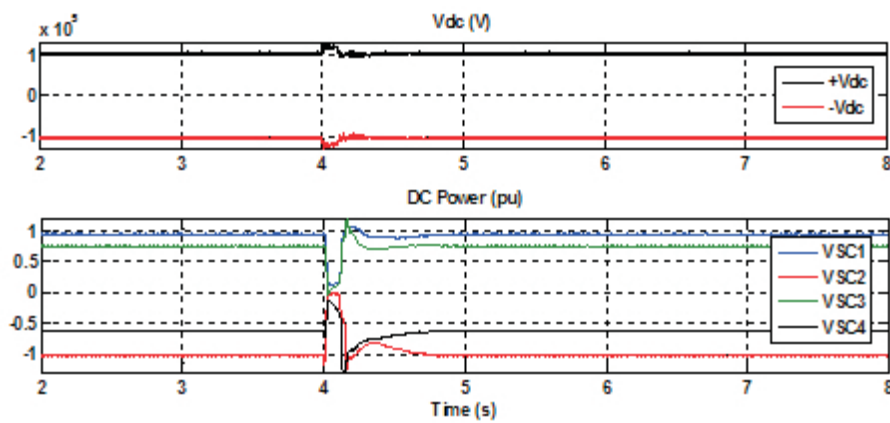
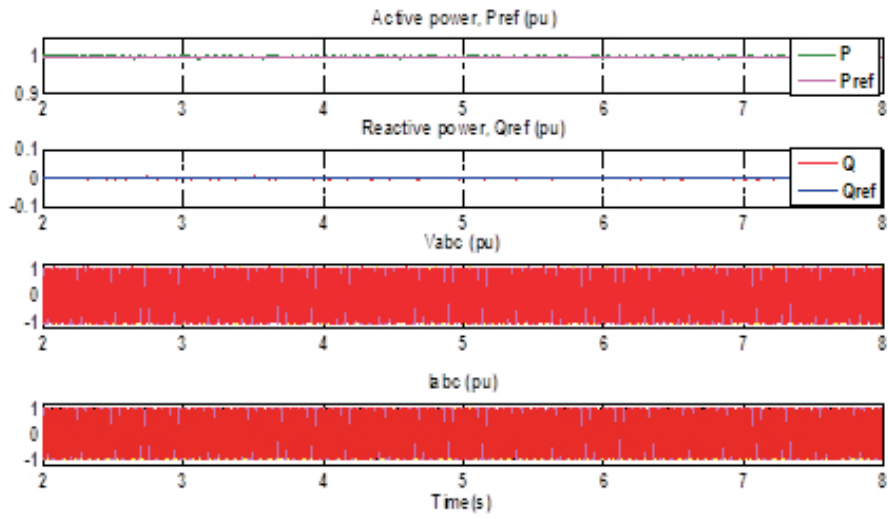
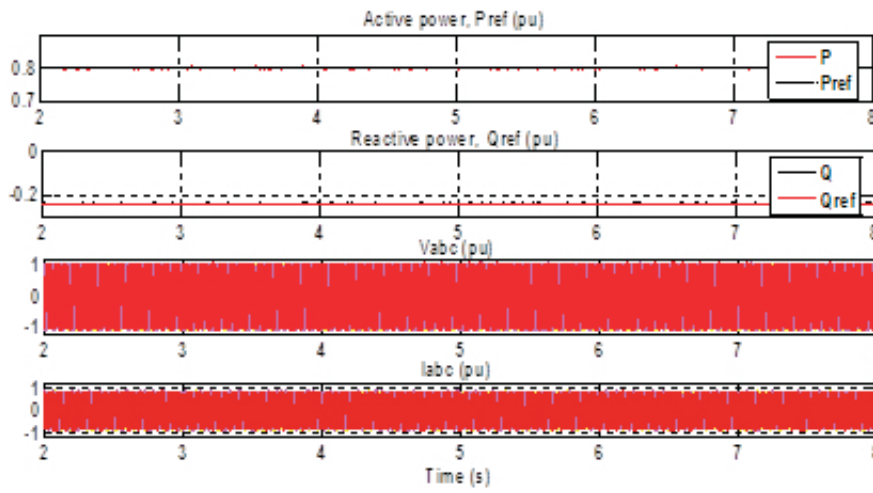


**Figure 4:** Dynamics of (a) VSC1 (b) VSC2 (c) VSC3 (d) VSC4 (e) Wind farm and (f) DC link parameters for a 3-phase fault at onshore AC grid with a duration of 5 cycles.

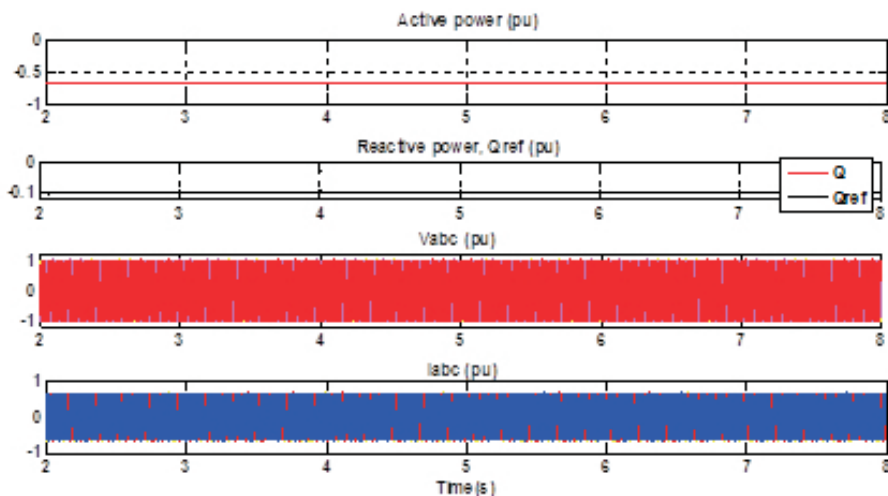
(a)



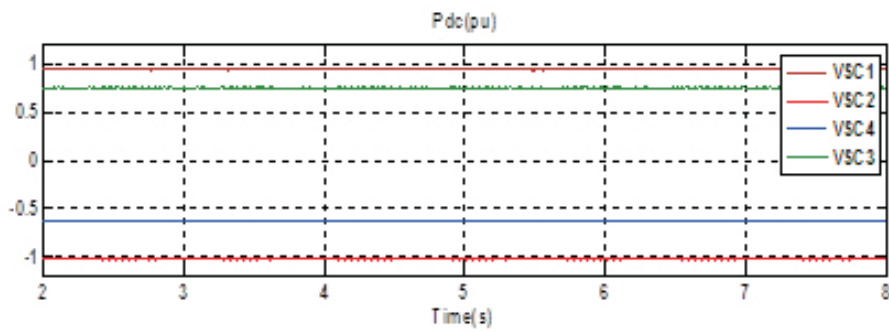
(b)



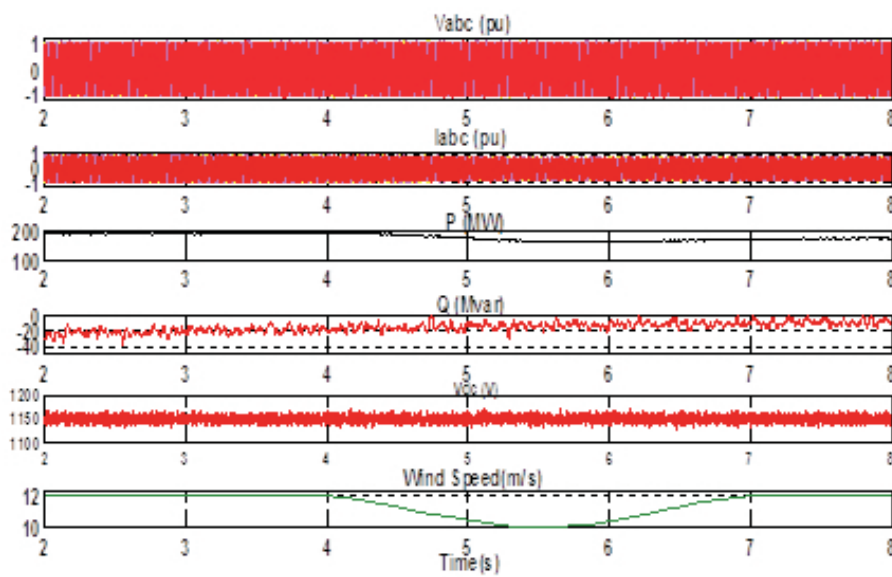
(c)



(d)



(e)



(f)

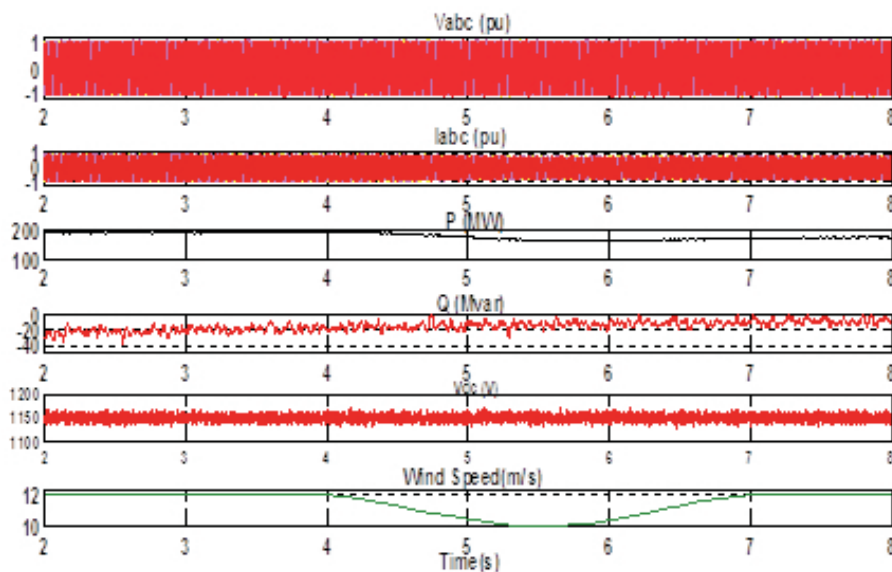
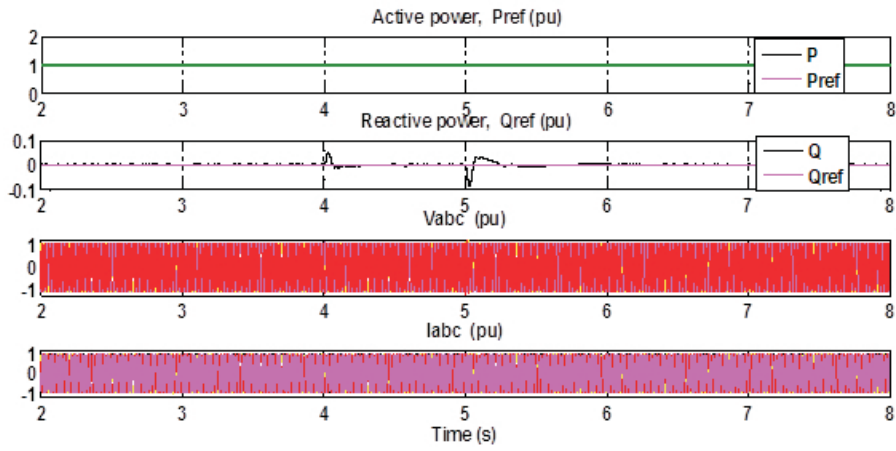
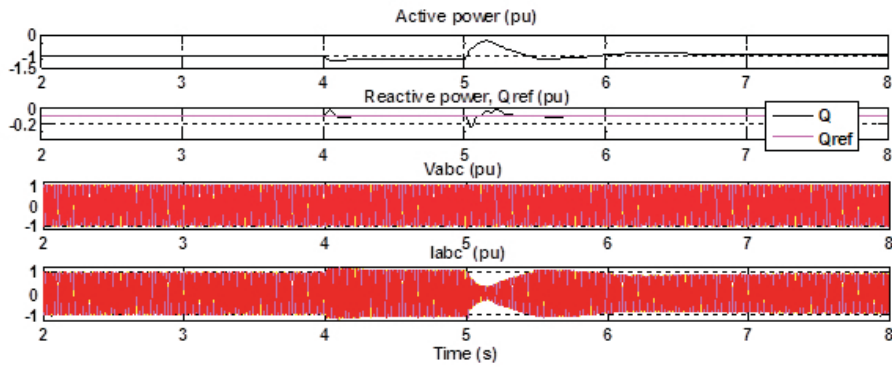


Figure 5: Dynamics of (a) VSC1 (b) VSC2 (c) VSC3 (d) VSC4 (e) DC powers and (f) Wind farm parameters for a change in wind speed.

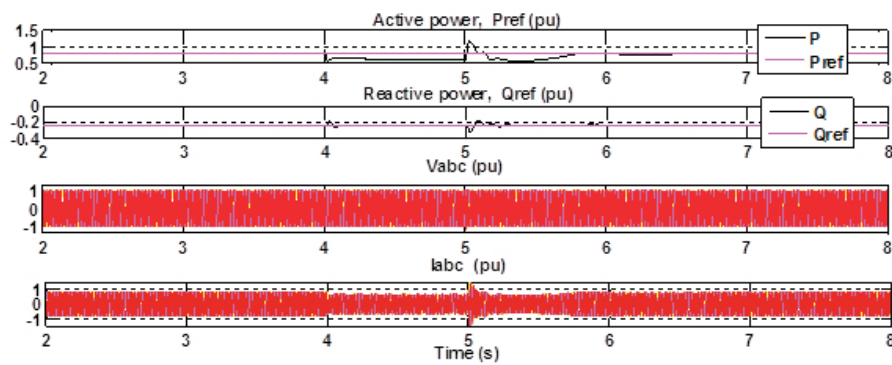
(a)



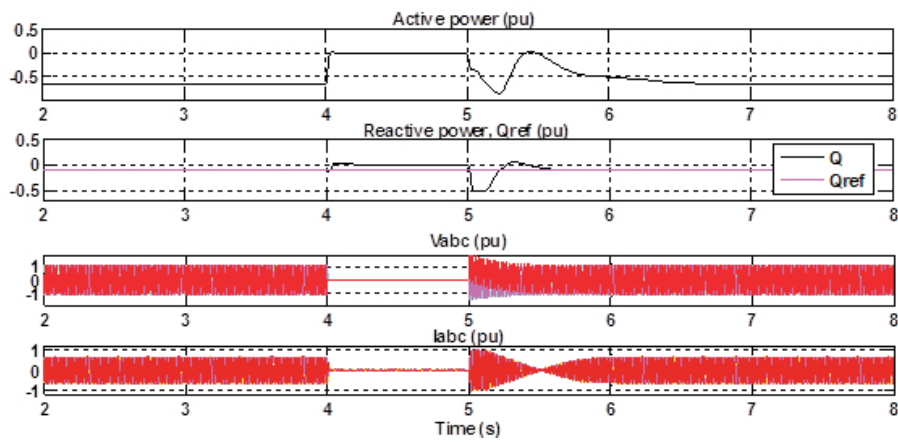
(b)



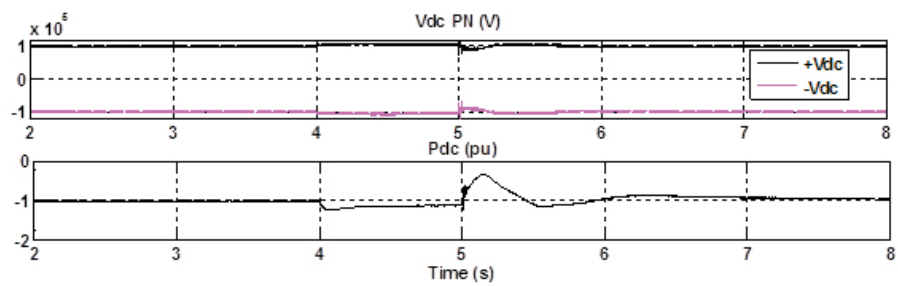
(c)



(d)



(e)



(f)

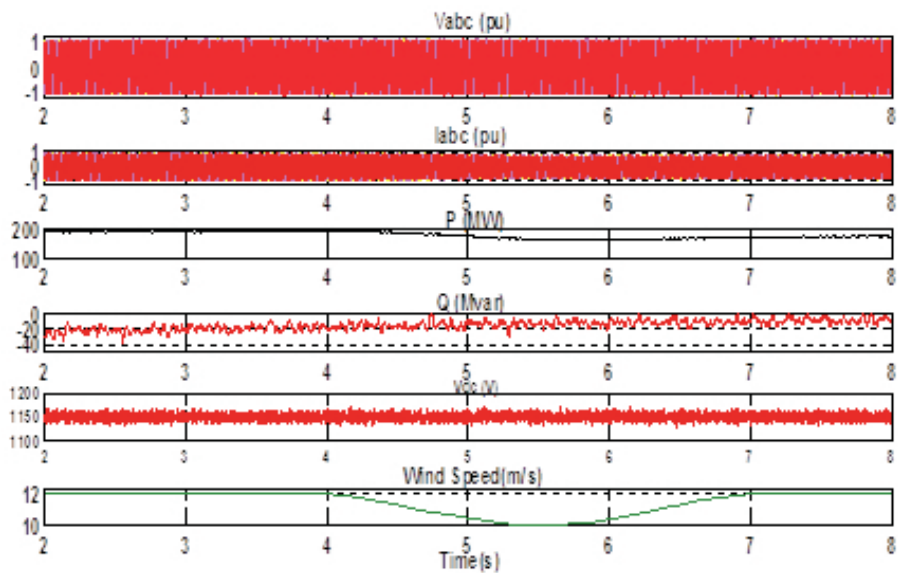


Figure 6: Dynamics of (a) VSC1 (b) VSC2 (c) VSC3 (d) VSC4 (e) DC link of VSC 2 and (f) Wind farm parameters for a converter outage (VSC4).

### 3.3 Offshore Converter Outage (VSC4)

Finally, to show the potential benefits of the VSC MTDC system in terms of security and reliability the loss of one converter is investigated. In this case study, offshore converter VSC4 is intentionally isolated from the system at  $t = 4$  sec and reconnected at  $t = 5$  sec. The simulation results obtained for temporary loss of offshore oil platform converter are shown in Figure 6. One can be noticed that during the outage of VSC4, the power is bypassed to the onshore AC grid through the converter VSC3 without violating the converter power ratings and hence the MTDC system maintains stability as depicted in Figure 6 (a) - (d). The DC link voltage of converter VSC3 is maintained constant at 1 pu with very little overshoot in its transient response as shown in Figure 6 (e). But the wind farm parameters depicted in Figure 6 (f) are not affected from the converter outage. ANFIS based controller coordinates the MTDC system in such a way that no converter has violated its power ratings and the whole system satisfies the power balance equation.

## 4 Conclusions

This paper has investigated the ANFIS based coordinated control strategy of MTDC system dealing with offshore VSCs and onshore VSCs for different perturbations. The simulation results under normal condition shows that the coordinated control strategy keeps AC voltage RMS constant, transmits the power from wind farms to AC grid and offshore oil platform via DC line. Similarly, for large perturbations at an AC grid/ offshore platform, the MTDC system responds quickly and then each controlled output returns to its pre-defined value immediately. Another advantage of MTDC system operation in integrating offshore wind farms to the onshore grid is that, when parts of the system are separated due to various reasons, the MTDC system continues to operate in the stable region without violating its converter power ratings. Hence, the proposed adaptive coordinated controller is able to maintain the stability and reliability by just its learning ability without following any mathematical procedure.

## References

- [1] Ajay Kumar M., Archana K. U., Srikanth N. V., HVDC Light Systems: An overview, *Int. Rev. Model. Simul.*, 2012, 5, 1951-1959.

- [2] Lu W., Ooi B. T., Premium quality power park based on multiterminal HVDC, *IEEE T. Power Deliver.*, 2005, 20, 978-983.
- [3] Vrionis T. D., Koutiva X. I., Giannakopoulos G. B., Control of an HVDC link connecting a wind farm to the grid for fault ride-through enhancements, *IEEE T. Power Syst.*, 2007, 22, 2039-2047.
- [4] Tang L., Ooi B.T., Protection of VSC-multi-terminal HVDC against DC faults, In: *Proceedings of IEEE Annual Power Electronics Specialists Conference (23-27 June 2002, Cairns, Queensland, Australia)*, IEEE, 2002, 719-724.
- [5] Hairong C., Chao W., Fan Z., Wulue P., Control strategy research of VSC based multiterminal HVDC system, In: *Proceedings of IEEE PES Power Systems Conference and Exposition (29 October - 1 November 2006, Atlanta, Georgia, USA)*, IEEE, 2006, 1986-1990.
- [6] Cole S., Beerten J., Belmans R., Generalized dynamic VSC MTDC model for power system stability studies, *IEEE T. Power Syst.*, 2010, 25, 2010, 1655-1662.
- [7] Ajay Kumar M., Srikanth N. V., Fast Fault Recovery of a Grid Integrated Wind Farm Based HVDC Light Transmission System with ANFIS controller, *Russ. Electr. Eng.*, 2014, 85, (In press).
- [8] Xu L., Fan L., Miao Z., Modeling and Simulation of Multi-Terminal HVDC for Wind Power Delivery, In: *Proceedings of IEEE Power Electronics and Machines in Wind Applications (16-18 July 2012, Denver, Colorado, USA)*, IEEE, 2012, 1-6.
- [9] Lie X., Liangzhong Y., Bazargan M., DC grid management of a multi-terminal HVDC transmission system for large offshore wind farms, In: *Proceedings of the 1st International Conference on Sustainable Power Generation and Supply 6-7 April 2009, Nanjing, China*, Power Network Technology Press, 2009, 1-7.
- [10] Kirby N. M., Xu L., Luckett M., Siepmann W., HVDC transmission for large offshore wind farms, *IEEE T. Power Eng. J.*, 2002, 16, 135-141.
- [11] Zhu J., Booth C. D., Adam G. P., Roscoe A. J., Bright C. G., Inertia emulation control strategy for VSC-HVDC transmission systems, *IEEE T. Power Syst.*, 2013, 28, 1277-1287.
- [12] Dierckxsens C., Srivastava K., Reza M., Cole S., Beerten J., Belmans R., A distributed DC voltage control method for VSC MTDC systems, *Electric Power Syst. Res.*, 2012, 82, 54-58.
- [13] Yin S., Yang X, Karimi H. R., Data-driven adaptive observer for fault diagnosis, *Math. Prob. Eng.*, 2012, 2012, 194-199.
- [14] Ajay Kumar M., Srikanth N. V., Modelling and simulation of SVPWM based vector controlled HVDC Light systems, *Leonardo Electronic Journal of Practices and Technologies*, 2012, 11, 23-36.
- [15] Ajay Kumar M., Srikanth N. V., An adaptive neuro fuzzy inference system controlled space vector pulse width modulation based HVDC Light transmission system under AC fault conditions, *Cent. Eur. J. Eng.*, 2014, 4, 27-38.
- [16] Wang L., Truong D.-N., Stability enhancement of a power system with a PMSG-based and a DFIG-based offshore wind farm using a SVC with an adaptive-network-based fuzzy inference system, *IEEE T. Ind. Electron.*, 2013, 60, 2799-2807.